First-Principles-Based Predictive Simulations of B Diffusion and Activation in Ion Implanted Si

Silva K. Theiss, Maria-Jose Caturla, Thomas J. Lenosky, Babak Sadigh, and Tomas Diaz de la Rubia
University of California, Lawrence Livermore National Laboratory, Livermore, CA 94550

Martin D. Giles
Intel Corporation, Santa Clara, CA 95051

Majeed A. Foad
Applied Materials Corporation, Santa Clara, CA 95054

Abstract- We present a kinetic Monte Carlo model for boron diffusion, clustering and activation in ion implanted silicon. The input to the model is based on a combination of experimental data and *ab initio* calculations. The model shows that boron diffusion and activation are low while vacancy clusters are present in the system. As the vacancy clusters dissociate, boron becomes substitutional and the active fraction increases rapidly. At the same time, the total boron diffusion length also increases rapidly while interstitial clusters ripen. The final burst of boron diffusion occurs as the large interstitial clusters dissolve, but most of the transient diffusion of the implanted boron has already taken place by this time. We show that these results are in excellent agreement with experimental data on annealed dopant profiles and dopant activation as a function of annealing time.

I. INTRODUCTION

Ion implantation is the most commonly used method of selectively doping Si with the fine depth control required for integrated circuit applications. In current and near-future device generations, p-type source and drain regions of MOSFETS are created by implanting B ions at energies that range from a few tens of keV down to a few tenths of a keV. However, the highly energetic incident ions damage the Si lattice, creating vacancies and interstitials far in excess of their equilibrium concentrations. Further, most of the B is not initially electrically active. Thus, to eliminate the damage and to electrically activate the B, the Si wafer must be annealed. However, B diffuses by binding to a Si interstitial (I) [1], so the excess I concentration during this anneal leads to B diffusion orders of magnitude faster than in equilibrium. This transient enhanced diffusion (TED) causes B to diffuse both deeper into the Si, increasing the junction depth, and laterally under the gate, changing the channel length. Additionally, in the presence of an excess interstitial concentration, B forms clusters at concentrations below its equilibrium solid solubility. This severely limits the concentration of electrically active B that can be achieved. Thus the challenge for future device generations is two-fold: to minimize the TED and to maximize the electrical activity of the implanted B.

The diffusion of B has been extensively studied by a variety of theoretical techniques [2-4] and is now well understood. Substitutional B^- binds to a Si interstitial (I) to form the mobile complex BI^+ with a binding energy of 0.9 eV. This complex can either diffuse as an interstitialcy via the hexagonal site in the diamond cubic lattice with a migration energy of about 0.7 eV, or dissociate, with a kinetic barrier of about 1.8 eV (0.9 eV binding energy plus 0.9 eV migration energy of I.) [2] Since dissociation is less favorable than migration, mobile B makes many diffusive hops before becoming immobile again through dissociation [5]. Thus the diffusion length of a boron interstitialcy is reduced at higher temperatures, where dissociation becomes less unfavorable with respect to migration.

By contrast, the clustering of B with Si interstitials is a very complex problem and is not well understood. We have exhaustively studied the energetics of small B clusters using *ab intio* density functional theory [6]. The results of the *ab initio* calculations, along with molecular

0-7803-6279-9/00/$10.00 © 2000 IEEE

dynamics (MD) simulations and fundamental experiments, are then used as input to kinetic Monte Carlo (kMC) simulations of B implantation and annealing. The diffusion and electrical activation predicted by these simulations are validated against controlled experiments.

KMC has been used extensively in recent years to study defect and impurity diffusion in irradiated materials [7-9]. In silicon, the Bell Labs group has done extensive work in this area and has had great success in simulating a wide variety of experimental results. In our approach, we attempt to minimize the number of free parameters in the model by using *ab initio* calculations to determine the energetics and diffusion barriers of the key diffusing species in the model. By using experiments to validate the results, the outcome should be a physically-based predictive model.

II. KINETIC MONTE CARLO MODEL AND INPUT DATA

The basic kMC model used in this work has been described previously [10]. Briefly, it tracks the locations of defects, dopants, impurities, and extended defects (clusters) as a function of time. At each time step, we randomly choose among all possible events in the simulation box. The probability of each event is set by its rate, which is determined by the energy and prefactor (entropy) associated with the event. Then the simulation time is incremented by the inverse of the sum of the rates for all possible events in the simulation box. (Thus the model takes longer time steps when fewer events can occur.) Because kMC focuses only on important particles and events, time scales of hours can be reached with these simulations.

In order to generate the necessary input files for the kMC simulation, we need to know the migration mechanisms, energies, and prefactors for the mobile species, which in our model are BI, I, and V. Additionally, we need to know the binding energies and dissociation prefactors for all the relevant defect and dopant-defect clusters. Clearly, it is an impossible task to calculate or obtain from experiment all the energy barriers and entropies associated with all possible reactions. Moreover, it is also clearly impossible to know what all the possible reactions may be for a given set of defects, dopants, impurities, sources and sinks. Thus, one of the roles of a KMC model is to determine which are the reactions and energetics that play an important role in determining the final profile and activation state. As we shall see below, the model developed here is rather successful in this endeavor.

The migration energies of the mobile species considered are given in Table 1. The migration energies of silicon interstitials and vacancies, and the binding energies of pure interstitial and vacancy clusters were determined by MD simulations [11] for small clusters. For larger clusters, the binding energies were obtained [11] by a fit between the values for small clusters and the experimental value for dissociation of {311} defects [12] for the interstitial clusters and the theoretical value for vacancy formation energy [12] for the vacancy clusters. The diffusion barrier and mechanism and of the B interstitialcy was determined from *ab initio* calculations as described above [2].

TABLE I
Migration energies and pre-factors for the species considered in the kMC simulations * Value obtained from fitting the experimental data of Boron diffusivity [17]

Species	Pre-factor (cm^2/s)	Migration Energy (eV)	Reference
V	10^{-3}	0.43	[11]
I	10^{-2}	0.9	[11]
BI	$4x10^{-6}$ *	0.68	[2]

The binding energies and charge states for small B-I clusters were obtained by *ab initio* calculations in the local density approximation. The most stable cluster in this range is the $B3I^-$, which consists of two B atoms on near-substitutional sites with another B on the bond-center between them. The unique ability of *ab initio* calculations to identify the lowest energy charge state, as well as the lowest energy structure, is critical in the case of small B clusters. The charge of a cluster determines both how a cluster contributes to the doping level (e.g., $B3I^-$ negates the doping effect of two of the

B atoms), and how that cluster will attract or repel the charged mobile species and thus how likely it is to grow. Binding energies of boron clusters are give in reference [6].

For interstitial-rich B clusters, it was assumed that the energy required to remove an interstitial from a cluster was not changed by the presence of a B atom in the cluster. Thus the binding energy of an I to a Bn_BIn_I cluster was taken to be the same as to an $I(n_B+n_I)$ cluster. This assumption then determined the binding energy of BI^+ to these clusters.

Because it is impossible to calculate the binding energies of very large clusters from first principles, we made a set of assumptions based on our understanding of the binding of small clusters. The key insight is the fact that B3I is a very stable complex. Moreover, it is known from the phase diagram that boron in silicon at high concentrations precipitates into a B_3Si line compound with the same stochiometry as the B3I complex. Thus, for B-rich clusters larger than B4I2, it was assumed that the dissolution energies in the vicinity of B6I2 repeated the pattern around B3I. (e.g., the energy required to remove a BI from B6I2 equals that to remove it from B3I; the energy to remove a BI from B5I2 equals that to remove it from B2I, etc.) The only exception was the binding energy of BI to B5I2, which was arbitrarily increased by 0.4 eV above the binding energy of BI to B2I, so that the clusters in the $B5In_I$ column would in general be more energetically favorable than those in the $B4In_I$ column. This scheme probably underestimates the binding energies of the larger clusters to some degree, but we found this not to be particularly important in the context of the final results.

Clusters of size up to B7I10 are included in the input files. If a mobile BI^+ joins a B cluster which already has 7 B atoms, the cluster is broken up into B6I2 plus an appropriate remainder. (i.e., $B7In_I$ + BI -> B6I2 + $B2I(n_I-1)$.) This was done so that there are no clusters that are "invisible" to mobile BI but the number of input species does not become too large to handle. The number of clusters that grow to have more than six B atoms is a small fraction of the total in the simulations discussed here and therefore we do not expect this approximation to effect the final results. Additionally, BI is allowed to join any interstitial or vacancy cluster. Interstitial clusters up to size 300 and vacancy clusters up to size 100 are included in the simulation. If three BI join an interstitial cluster, it is broken up into B3I plus an appropriately sized interstitial cluster. (BI + $B2In_I$ -> B3I + In_I.) The assumption is that it is relatively easy for B to diffuse along the boundaries of an interstitial cluster and form a more stable structure. Again, this approximation is made so that the number of input species is not too large. Up to three BI may join any given vacancy cluster. Additional BI simply do not react in the current model. Again, the number of clusters for which this becomes an issue is small in these simulations.

The model currently assumes that B in a V cluster is electrically inactive, as B on a surface is. This is expected to be a good assumption for large V clusters. However, our *ab initio* calculations show that B in a V6 cluster is actually electrically active. The exact break point between clusters in which the B is negatively charged and those in which it is neutral is not known, but for simplicity we assumed it neutral in all V clusters. It is also known that substitutional B does not bind vacancies, so when clusters dissolve to the point where only one vacancy is left the vacancy immediately hops away.

III. RESULTS

Fig. 1 shows simulated and experimental B diffusion profiles following a 40 keV implant of B to a dose of $2x10^{14}$ ions/cm^2 and anneals at 700, 800, or 900° C. The simulations follow the trends in the experimental data very well and show the fraction of boron clusters near the peak of the implant profile. This clustering of boron is responsible for the break in the diffusion profile observable between 200 and 300 nm that results in the long transient diffusion tail. Because we know the charge state of the boron clusters from the results of our *ab*

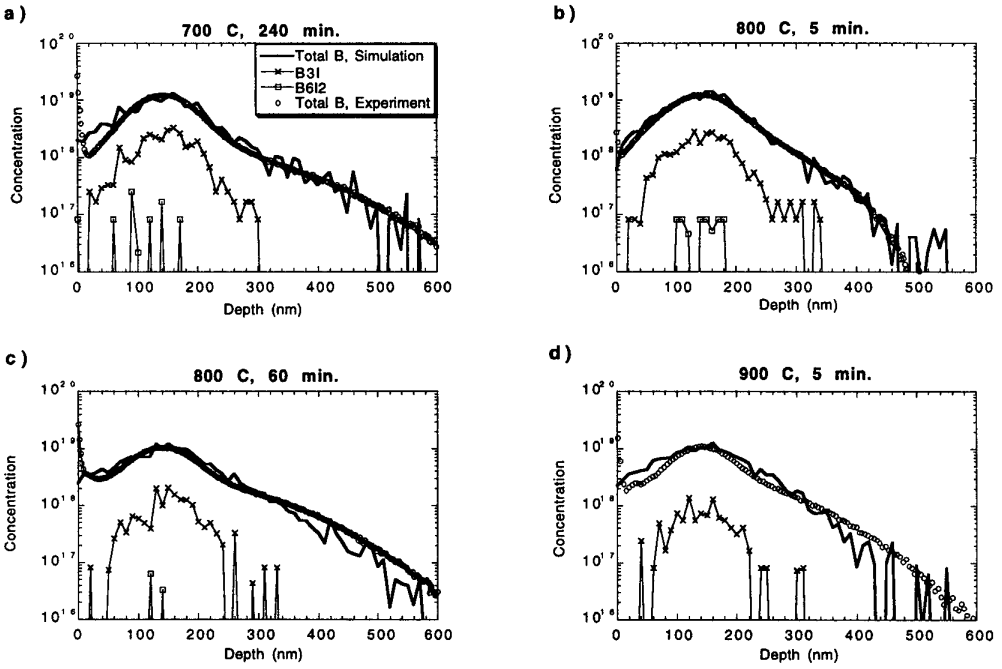

Fig. 1. Depth concentration profiles for 40 keV Boron implantation at a dose of $2x10^{14}$ ions/cm^2. Solid lines are the total Boron concentration from the kMC simulation. Open squares are the SIMS profiles. The most important Boron clusters are also shown (B3I). Termperatures and times are: (a) 700•C for 240 minutes, (b) 800•C for 5 minutes, (c) 800•C for one hour and (d) 900•C for 5 minutes.

initio calculations, we are able to calculate the fraction of active boron as a function of annealing time. Fig. 2 shows the simulated and experimental electrically active B fractions as a function of time for an anneal at 800 C of the 40 keV ion implanted boron profile. The circles labeled Experiment 1 are spreading resistance profilometry data measured at Applied Materials Corporation. The x's labeled Experiment 2 are from ref.[13]. The simulation reproduces the shape of the experimental data quite well: it is flat for the first 10 s of the anneal, then increases with time. The rate of increase after 10 s appears to be slightly too fast compared to experiment. Suggesting that the binding energy of some of the important B-I clusters may be too low in our simulation.

The reason for the change in slope near 10 s can be seen in Fig. 3. This is a plot of the average size of the vacancy and intersitial clusters in the system as a function of time, and also shows the total B diffusion distance as a function of time on the right axis. The average vacancy cluster size peaks around 20 s and then drops as the vacancies are eliminated from the system. As the vacancy clusters dissolve, any B trapped in them becomes active.

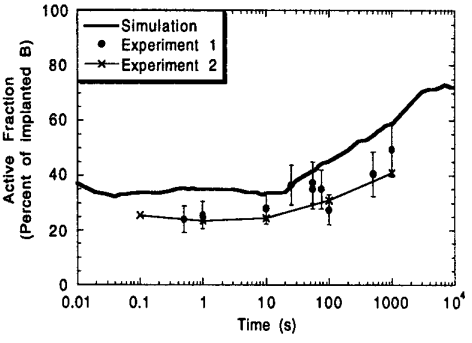

Fig. 2 Active fraction of Boron from kMC simulations (solid line) and from two different experiments (•) Applied Materials

From Fig. 3 we can also see that the bulk of TED occurs during the growth phase of the interstitial clusters, not during their dissolution. Out of a total of about 100 nm of TED in this system at 800 C, about 15 nm occur while vacancies are present in the system, 50 nm occur as the interstitial clusters are ripening, and 35 nm occur during the final dissolution of the interstitial clusters. This is in agreement with our predictions based on earlier versions of the kMC model [14] and shows that the bulk of TED occurs before the final dissolution of the Si interstitial clusters.

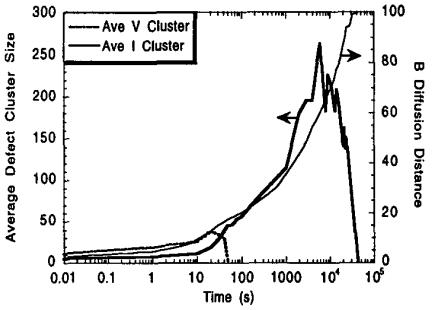

Fig. 3 Evolution of vacancy (dashed line) and interstitial (solid line) clusters during annealing at 800•C, (left axis). The distance traveled by the B atoms during annealing is also shown (thin solid line, right axis). Notice that most of the Boron diffusion occurs when vacancies have dissapeared.

IV. CONCLUSIONS

We have developed a model for Boron diffusion and clustering based on first principles calculations of cluster binding energies and migration. This model can reproduce the experimental SIMS profiles of Boron concentration for different temperature annealing conditions, as well as the Boron active fraction as a function of time during the anneal. The model shows that most of the diffusion occurs during the growth of interstitial clusters, when all vacancies have recombined with other interstitials or the surface.

ACKNOWLEDGMENTS

This work was performed under the auspices of the US Department of Energy by Lawrence Livermore National Laboratory under contract W-7405-Eng-48.

REFERENCES

[1] U. Gösele and H. Strunk, Appl. Phys. **20,** 263 (1979); A. Antoniadis and I. Moskowitz, J. Appl. Phys. **53,** 6788, (1982)

[2] J. Zhu, T. Diaz de la Rubia, L. H. Yang, C. Mailhiot, G. H. Gilmer, Phys. Rev. **B54**, 4741 (1996)

[3] B. Sadigh, T. J. Lenosky, S.K. Theiss, M.-J. Caturla, T Diaz de la Rubia, M.A. Foad, Phys. Rev. Lett., **83**, (1999) p.4341

[4] W. Windl, M. M. Bunea, R. Stumpf, S. T. Dunham, and M. P. Masquelier, Phys. Rev. Lett., **83**, (1999) p.4344

[5] N.E.B. Cowern, K.T.F. Janssen, G.F.A. van de Walle, D. J. Gravesteijn, Phys. Rev. Lett. **65**, 2434 (1990)

[6] T. J. Lenosky, B. Sadigh, S. K. Theiss, M.-J. Caturla, and T. Diaz de la Rubia, Appl. Phys. Lett. (to be published)

[7] H. L. Heinisch, Nucl. Instrum. and Methods **B102,** 47 (1995)

[8] M. Jaraiz, G. H. Gilmer, J. M. Poate, Appl. Phys. Lett. **68,** 409 (1996)

[9] M. D. Johnson, M.-J. Caturla, T. Diaz de la Rubia, J. Appl. Phys. **84** (1998) 1963

[10] M.-J. Caturla, Comput. Mater. Sci., **12** (1998) 319

[11] G. H. Gilmer, T. Diaz de la Rubia, D. M. Stock and M. Jaraiz, Nucl. Instrum. and Methods **B102**, 247 (1995)

[12] P.A. Stolk, H. J. Gossmann, D.J. Eaglesham, D.C. Jacobson, J.M. Poate, Appl. Phys. Lett. **66**, 568 (1995); C. S. Rafferty, G. H. Gilmer, M. Jaraiz, D. Eaglesham, H.-J. Gossmann, Appl. Phys. Lett. **68**, 2395 (1996)

[13] L. Pelaz, G.H. Gilmer, H.-J. Gossmann, C.S. Rafferty, M. Jaraiz, J. Barbolla, Applied Physics Letters, **74** (1999) p.3657; L.A. Pelaz, V.C. Venezia, H.-J. Gossmann, G.H. Gilmer, A.T. Fiory, C.S. Rafferty, M. Jaraiz, J. Barbolla, **75**, (1999) p.662

[14] M.-J. Caturla, M. D. Johnson, T. Diaz de la Rubia, App. Phys. Lett., **72** (1998) p.2736-8

[15] A.D. Kurtz, R. Yee, J. Appl. Phys. 31 (1960) p.303